Demonstration of the Role of Scission of the Proximal Histidine−Iron Bond in the Activation of Soluble Guanylyl Cyclase through Metalloporphyrin Substitution Studies§

Elizabeth A. Dierks,† Songzhou Hu,‡ Kathleen M. Vogel,‡ Anita E. Yu,† Thomas G. Spiro,‡ and Judith N. Burstyn*,†

Contribution from the Department of Chemistry, University of Wisconsin, Madison, Wisconsin 53706, and Department of Chemistry, Princeton University, Princeton, New Jersey 08544

Received January 29, 1996. Revised Manuscript Received March 23, 1997⊗

Abstract: Activation of soluble guanylyl cyclase (sGC) by NO correlates with scission of the proximal iron−histidine bond, as demonstrated by the application of electronic absorption and resonance Raman spectroscopy to the study of metalloporphyrin-substituted enzymes. The non-native metalloporphyrins, Mn(II)PPIX and Co(II)PPIX, can be introduced into heme-deficient sGC forming five-coordinate complexes. The similarity among Mn(II)sGC, Co(II)-sGC, and the corresponding metalloporphyrin-substituted derivatives of Mb and Hb provides confirming evidence for the presence of an axial histidine ligand in sGC. Upon addition of NO, Mn(II)sGC forms a six-coordinate species with the histidine ligand still bound to the Mn, and the enzyme is not activated. In contrast, the Co(II)-sGC(NO) adduct is five-coordinate and the enzyme is activated. These data imply that the activated state of sGC is attained when the proximal histidine−metal bond is broken.

Soluble guanylyl cyclase (sGC), the cytosolic enzyme that catalyzes the conversion of guanosine 5′-triphosphate (GTP) to guanosine 3′,5′-monophosphate (cGMP), is the only proven biological receptor for nitric oxide.[1−3] Nitric oxide (NO) is an unique messenger molecule being both freely diffusible and highly labile; consequently, its action is limited to the immediate environment in which it is released. NO is synthesized from L-arginine by the enzyme NO-synthase and regulates vascular smooth muscle relaxation, inhibition of platelet aggregation, and neuronal communication.[4,5] NO controls these functions through activation of sGC.[6] sGC is a 150 kDa heterodimer with subunits of similar size[7,8] and was believed to contain 1 mol of heme (Fe(II)PPIX) per mol of heterodimer.[9] Recent results suggest, however, that there may be one heme in each subunit.[10] Enzyme activity is dependent on the presence of a divalent metal ion cofactor Mg^{2+} (the natural cofactor) or Mn^{2+}, in excess of the substrate GTP.[1,2] Although the heme-free enzyme has basal activity, the addition of heme is absolutely required for activation by NO.[1,11,12] Heme-containing sGC is activated both by NO[11,13] and by nitrosyl-heme (NO-heme);[2,14,15] NO-heme and the metal-free protoporphyrin IX (PPIX) also activate the heme-deficient enzyme.[2,16,17] The mechanism of enzyme activation is not yet understood.

Recent spectroscopic studies[18−22] confirm that NO binds directly to the Fe atom in the heme group to form NO-heme, implicating this species in the activation process. These studies indicate that the resting form of sGC is either five-coordinate Fe(II)PPIX(His)[18,22] or a mixture of five-coordinate Fe(II)PPIX-(His) and six-coordinate Fe(II)PPIX$(His)_2$.[19,20] NO-activated sGC has been shown to contain a five-coordinate Fe(II)PPIX-

† University of Wisconsin.

‡ Princeton University.

§ Abbreviations: Fe(II)PPIX (heme), iron(II) protoporphyrin IX; Mn-(II)PPIX, manganese(II) protoporphyrin IX; Co(II)PPIX, cobalt(II) protoporphyrin IX; sGC, soluble guanylyl cyclase; GTP, guanosine 5′-triphosphate; cGMP, guanosine 3′,5′-cyclic monophosphate; TEA, triethanolamine·HCl; DTT, D,L-dithiothreitol; PEI-F, polyethyleneimine cellulose with fluorescent indicator; TLC, thin layer chromatography; SNAP, *S*-nitroso-*N*-acetylpenicillamine; PEG, polyethylene glycol; ATP, adenosine 5′-triphosphate; Hb, hemoglobin; Mb, myoglobin; CCP, cytochrome *c* peroxidase; 2-MeImH, 2-methylimidazole; cyt *c*, cytochrome *c*; HRP, horseradish peroxidase; ImH, imidazole; OEP, octaethylporphyrin; PPIXDME, protoporphyrin IX dimethyl ester; SNP, sodium nitroprusside; RR, resonance Raman spectroscopy; Pip, piperidine; Py, pyridine; 4-MePip, 4-methylpiperidine; Mn(II)sGC, Mn(II)PPIX-reconstituted sGC; Fe(II)sGC, Fe(II)-PPIX-reconstituted sGC; Co(II)sGC, Co(II)PPIX-reconstituted sGC; TPP, α,β,γ,δ-tetraphenylporphyrin.

⊗ Abstract published in *Advance ACS Abstracts,* July 1, 1997.

(1) Ignarro, L. J.; Degnan, J. N.; Baricos, W. H.; Kadowitz, P. J.; Wolin, M. S. *Biochim. Biophys. Acta* **1982**, *718*, 49−59.

(2) Wolin, M. S.; Wood, K. S.; Ignarro, L. J. *J. Biol. Chem.* **1982**, *257*, 13312−13320.

(3) Waldman, S. A.; Murad, F. *Pharmacol. Rev.* **1987**, *39*, 163−196.

(4) Stuehr, D. J.; Griffith, O. W. *Adv. Enzymol. Relat. Areas Mol. Biol.* **1992**, *65*, 287−386.

(5) Bredt, D. S.; Snyder, S. H. *Ann. Rev. Biochem.* **1994**, *63*, 175−195.

(6) Ignarro, L. J. *Seminars Hematology* **1989**, *26*, 63−76.

(7) Garbers, D. L. *J. Biol. Chem.* **1979**, *254*, 240−243.

(8) Kamisaki, Y.; Saheki, S.; Nakane, M.; Palmieri, J. A.; Kuno, T.; Chang, B. Y.; Waldman, S. A.; Murad, F. *J. Biol. Chem.* **1986**, *261*, 7236−7241.

(9) Gerzer, R.; Böhme, E.; Hofmann, F.; Schultz, G. *FEBS Lett.* **1981**, *132*, 71−74.

(10) Stone, J. R.; Marletta, M. A. *Biochemistry* **1995**, *34*, 14668−14674.

(11) Craven, P. A.; DeRubertis, F. R. *J. Biol. Chem.* **1978**, *253*, 8433−8443.

(12) Craven, P. A.; DeRubertis, F. R. *Biochim. Biophys. Acta* **1983**, *745*, 310−321.

(13) Gruetter, C. A.; Barry, B. K.; McNamara, D. B.; Gruetter, D. Y.; Kadowitz, P. J.; Ignarro, L. J. *J. Cycl. Nucl. Res.* **1979**, *5*, 211−224.

(14) Ohlstein, E. H.; Wood, K. S.; Ignarro, L. J. *Arch. Biochem. Biophys.* **1982**, *218*, 187−198.

(15) Ignarro, L. J.; Ballot, B.; Wood, K. S. *J. Biol. Chem.* **1984**, *259*, 6201−6207.

(16) Ignarro, L. J.; Wood, K. S.; Wolin, M. S. *Proc. Natl. Acad. Sci. U.S.A.* **1982**, *79*, 2870−2873.

(17) Ignarro, L. J.; Adams, J. B.; Horwitz, P. M.; Wood, K. S. *J. Biol. Chem.* **1986**, *261*, 4997−5002.

(18) Stone, J. R.; Marletta, M. A. *Biochemistry* **1994**, *33*, 5636−5640.

(19) Yu, A. E.; Hu, S.; Spiro, T. G.; Burstyn, J. N. *J. Am. Chem. Soc.* **1994**, *116*, 4117−4118.

(20) Burstyn, J. N.; Yu, A. E.; Dierks, E. A.; Hawkins, B. K.; Dawson, J. H. *Biochemistry* **1995**, *34*, 5896−5903.

(21) Stone, J. R.; Sands, R. H.; Dunham, W. R.; Marletta, M. A. *Biochem. Biophys. Res. Comm.* **1995**, *207*, 572−577.

(22) Denium, G.; Stone, J. R.; Babcock, G. T.; Marletta, M. A. *Biochemistry* **1996**, *35*, 1540−1547.

S0002-7863(96)00305-8 CCC: $14.00

(NO), indicative of displacement of the axial histidine ligand, by resonance Raman (RR),[19,22] electronic absorption,[9,18] and electron spin resonance (ESR) spectroscopy.[21] Carbon monoxide also binds to the heme in sGC, and magnetic circular dichroism (MCD)[20] and RR[19,22,23] spectroscopy demonstrate that the Fe(II)sGC(CO) is six-coordinate with His as the likely sixth ligand. There are conflicting reports on the effect of CO on enzyme function.[18,20,24] We find that CO does not activate sGC at a variety of physiologically relevant concentrations of CO and at a variety of heme concentrations.[20]

Both the spectroscopic and enzymological data are consistent with an activation mechanism in which the axial His ligand is displaced from the heme iron. Ignarro and co-workers[2] first proposed that the release of axial ligands from the heme iron could be the mechanism of activation based on their observation that PPIX activates heme-deficient sGC with similar kinetics and to the same extent as NO-heme. Traylor and Sharma amplified this proposal with thermodynamic[25] and experimental[26] data on model systems. The recent spectroscopic studies mentioned above support the axial ligand release mechanism since the NO-activated sGC contains five-coordinate Fe(II)-PPIX(NO),[9,19,21,22] whereas unactivated forms of sGC, Fe(II)-sGC, and Fe(II)sGC(CO) have the proximal iron−His bond intact.[18−20,22,27]

Model studies by Scheidt and co-workers have revealed an increasing trans influence of the NO ligand in the series Mn(II)TPP(NO)(L), Fe(II)TPP(NO)(L), and Co(II)TPP(NO)(L); as electrons are added to the metal center the metal−nitrogen bond trans to NO becomes progressively weaker.[28−33] Six-coordinate Mn(II)TPP(4-MePip)(NO)[29,30] and Fe(II)TPP(4-MePip)(NO)[28] were crystallized; the Fe−N bond to the axial ligand trans to NO was considerably longer than both the analogous Mn−N bond and the Fe−N bonds in other N-bound Fe(II) porphyrin complexes. Scheidt and co-workers were not able to crystallize six-coordinate Co(II)TPP(NO)(4-MePip), presumably because the cobalt has a low affinity for the sixth axial ligand.[31]

We sought to exploit the variable axial coordination in Mn, Fe, and Co porphyrin nitrosyl adducts to test the hypothesis that soluble guanylyl cyclase is activated upon binding NO by displacement of the proximal histidine from the coordination sphere of the heme iron. We hypothesized that Mn(II)PPIX-reconstituted sGC (Mn(II)sGC) would react with NO to form a six-coordinate adduct (Mn(II)sGC(NO)) with the proximal His bound to the Mn(II) since Mn(II)sGC(NO) is isoelectronic with Fe(II)sGC(CO) and the two species are expected to be isostructural. If axial ligand release is required for activation, then sGC would not be activated by Mn(II)sGC(NO) but would be activated by Co(II)sGC(NO), which is expected to remain five-coordinate. In the present study we have determined that the Mn- and Co-substituted enzymes have the predicted structures and that activation of guanylyl cyclase does indeed correlate with the scission of the metal-proximal ligand bond.

Experimental Methods

Materials. Q Sepharose Fast Flow, triethanolamine·HCl (TEA), D,L-dithiothreitol (DTT), benzamidine, ATP-agarose (9-atom spacer at C8), GTP-agarose (11-atom spacer at the ribose hydroxyl), polyethylene glycol (PEG), and hemin chloride were all purchased from Sigma. NO (99+%) was purchased from Liquid Carbonic. Sodium dithionite (purum, 99+%) was the highest quality available from Fluka Chemical. NaCl and NaOH were obtained from Fisher. $MgCl_2$, ammonium sulfate, and citric acid were obtained from Mallinckrodt. [α-^{32}P]GTP was from NEN-Dupont and EM Science PEI-F cellulose TLC plates were from VWR Scientific. Co(III)PPIXCl and Mn(III)PPIXCl were purchased from Porphyrin Products, Inc. Prepacked Sephadex G25 columns (PD-10) were purchased from Pharmacia.

Protein Isolation. Soluble guanylyl cyclase was isolated by a modification of the method reported previously.[34] Fresh bovine lung tissue was minced in a food processor, and the mince washed three times each with 1 mM EDTA, 25 mM TEA buffer, pH 7.8 and with 5 mM DTT, 25 mM TEA buffer, pH 7.8. The washed tissue was diluted to a final concentration of 40% (w/v) with 2 mM benzamidine, 5 mM DTT, 25 mM TEA buffer, pH 7.8. This mixture was then homogenized in a Waring blender. Following centrifugation at 13 000xg to pellet cell debris, the supernatant was stirred at 4 °C for 1 h with 1% polyethylene glycol (PEG). This solution was then centrifuged at 18 000xg for 1 h, and the supernatant batch adsorbed to Q Sepharose Fast Flow resin. The resin was vacuum-filtered and washed with 25 mM TEA, pH 7.8, 5 mM DTT, and 0.2 mM benzamidine three times. The resin was poured into a column (2.5 cm × 80 cm) and eluted with a 1.5-L salt gradient (0−0.7 M NaCl) in 0.2 mM benzamidine, 0.5 mg/L trypsin inhibitor, 0.5 mg/L leupeptin, 5 mM DTT, 25 mM TEA (pH 7.8) (TEA-DTT buffer). Active fractions from the ion exchange column were pooled and dialyzed against TEA-DTT buffer (pH 7.4) containing 1 mM $MgCl_2$. The dialysate was batch adsorbed onto ATP-agarose resin and then poured into a column and washed with TEA-DTT buffer (pH 7.4), 0.2 mM benzamidine, 1 mM $MgCl_2$. sGC was eluted with a 400 mL linear gradient of NaCl (0−0.7 M) in pH 7.4 TEA-DTT buffer at 75 mL/h. Active fractions were concentrated with an Amicon ultrafiltration cell (PM-30 membrane) and desalted on a PD-10 column into pH 7.4 TEA-DTT containing 0.2 mM benzamidine and 1 mM $MgCl_2$. The desalted sGC was then loaded onto a GTP-agarose column which was then washed with TEA-DTT (pH 7.4) containing 0.2 mM benzamidine and 1 mM $MgCl_2$. Finally, sGC was eluted with 0.7 M NaCl in TEA-DTT (pH 7.4) buffer. Active fractions were concentrated in an Amicon Centriprep-30 microconcentrator and stored at −80 °C. Purified sGC appeared on an SDS-PAGE gel as a tightly spaced pair of bands ($M_r \sim 70\,000$−$75\,000$) with one additional band at $M_r \sim 42\,000$. A 43 kDa contaminant in purified sGC has been observed previously and identified as actin.[35,36] The isolated sGC contained substoichiometric amounts of heme as measured by sensitivity of the enzyme to activation by 100 μM SNAP (41-fold activation) and by pyridine hemochromogen assay.[37]

Soluble Guanylyl Cyclase Assay. Soluble guanylyl cyclase activity was determined as described previously[34,38] by measurement of the formation of [^{32}P]cGMP from [α-^{32}P]GTP. The natural cofactor Mg^{2+} was used in all determinations of specific activity. Assay reactions contained 40 mM TEA buffer (pH 7.4), 10 mM DTT, 1 mM GTP, 3 mM Mg^{2+}, 0.3 mM IBMX, 2.5 pmol [α-^{32}P]GTP, and enzyme. The reaction was carried out at 37 °C for 10 min and quenched by addition of 0.5 mM EDTA on ice. The amount of [^{32}P]cGMP formed was quantitated by scintillation counting on a Beckman L-6000 scintillation counter following separation of [^{32}P]cGMP from [α-^{32}P]GTP by ion exchange TLC. Protein concentrations were determined by Biuret protein assay.[39] The basal specific activity of purified sGC was 86 nmol/mg/min. Due to the observed photolability of Mn(II)sGC(NO), Mn(II)sGC assays were carried out in the dark.

(23) Kim, S.; Deinum, G.; Gardner, M. T.; Marletta, M. A.; Babcock, G. T. *J. Am. Chem. Soc.* **1996**, *118*, 8769−8770.
(24) Brune, B.; Schmidt, K.-U.; Ullrich, V. *Eur. J. Biochem.* **1990**, *192*, 683−688.
(25) Traylor, T. G.; Sharma, V. S. *Biochemistry* **1992**, *31*, 2847−2849.
(26) Traylor, T. G.; Duprat, A. F.; Sharma, V. S. *J. Am. Chem. Soc.* **1993**, *115*, 810−811.
(27) Stone, J. R.; Marletta, M. A. *Biochemistry* **1995**, *34*, 16397−16403.
(28) Scheidt, W. R.; Brinegar, A. C.; Ferro, E. B.; Kirner, J. F. *J. Am. Chem. Soc.* **1977**, *99*, 7315−7322.
(29) Scheidt, W. R.; Hatano, K.; Rupprecht, G. A.; Piciulo, P. L. *Inorg. Chem.* **1979**, *18*, 292−299.
(30) Piciulo, P. L.; Rupprecht, G.; Scheidt, W. R. *J. Am. Chem. Soc.* **1974**, *96*, 5293−5295.
(31) Scheidt, W. R.; Hoard, J. L. *J. Am. Chem. Soc.* **1973**, *95*, 8281−8288.
(32) Scheidt, W. R.; Piciulo, P. L. *J. Am. Chem. Soc.* **1976**, *98*, 1913−1919.
(33) Scheidt, W. R.; Frisse, M. E. *J. Am. Chem. Soc.* **1975**, *97*, 17−21.
(34) Kim, T. D.; Burstyn, J. N. *J. Biol. Chem.* **1994**, *269*, 15540−15545.
(35) Mülsch, A.; Gerzer, R. *Methods in Enzymol.* **1991**, *195*, 355−363.
(36) Mülsch, A.; Gerzer, R. *Methods in Enzymol.* **1991**, *195*, 377−383.

Heme Depletion of sGC. Heme-depletion was carried out in order to prepare heme-deficient enzyme for NO-activation studies comparing native and non-native metalloporphyrin-reconstituted sGC. sGC was dialyzed against citric acid buffer (pH 5.5) containing 60% ammonium sulfate and the dialysate was then centrifuged at 13 000xg for 20 min. The pelleted protein was then redissolved in TEA-DTT buffer (pH 7.4) containing 0.2 mM benzamidine. Heme-depleted sGC contained no detectable heme by pyridine hemochromogen assay,[37] but it was activated slightly (2−8-fold) by 100 μM SNAP indicating that a small amount of heme was still present in the enzyme.

Reconstitution of sGC with Native and Non-Native Metalloporphyrins. All sGC samples were reconstituted with metalloporphyrin prior to resonance Raman and electronic absorption spectroscopic studies. Heme-depleted sGC was readily reconstituted anaerobically with Fe(II)PPIX, Mn(II)PPIX, and Co(II)PPIX. All metalloporphyrins were dissolved in 0.1 M NaOH and then diluted with TEA-DTT buffer (pH 7.4). A molar excess of a metalloporphyrin, previously reduced with sodium dithionite, was added to an anaerobic sample of heme-depleted sGC and stirred at room temperature for 15 min. The protein solution was desalted under nitrogen on a PD-10 column equilibrated with TEA-DTT buffer (pH 7.4) containing 0.2 mM benzamidine to remove any unbound metalloporphyrin. Metalloporphyrin-reconstituted sGC was characterized by electronic absorption spectroscopy and activity assay. The heme content of Fe(II)PPIX-reconstituted sGC was determined by pyridine hemochromogen assay.[37] The Co and Mn content of Co(II)sGC and Mn(II)sGC, respectively, was determined by atomic absorption spectrophotometry on a Perkin Elmer Model 3030 spectrophotometer with an HGA-300 furnace controller.

Preparation of the NO Adducts of Metalloporphyrin-Reconstituted sGC. Nitric oxide was generated for preparation of samples for resonance Raman spectroscopy by reaction of sodium nitrite (^{14}N- or ^{15}N-labeled) with sodium ascorbate in anaerobic solution. The gas was collected in a gas-tight syringe and was then added to the metalloporphyrin-reconstituted sGC to form the nitrosyl adduct. For preparation of samples for electronic absorption spectroscopy, a nitric oxide saturated solution was made by bubbling nitric oxide gas, purified by passage through a solid NaOH column and a solution of 6 N NaOH, through deoxygenated TEA buffer, pH 7.4. The saturated solution was then added to the metalloporphyrin-reconstituted sGC to form the nitrosyl adduct.

Spectrophotometric Measurements. Electronic absorption spectra of sGC were obtained in 25 mM TEA buffer, pH 7.4, containing 5 mM DTT and 0.2 mM benzamidine. Spectra were recorded on a Hitachi U-3210 spectrophotometer at concentrations of 5−15 μM sGC derivative. The millimolar absorptivities were calculated based on the measured Mn (for Mn(II)sGC) or Co (for Co(II)sGC) concentrations.

Resonance Raman Spectroscopy. RR spectra were acquired with a Spex 1877 triplemate spectrograph and detected with a cooled intensified diode array detection system (Princeton Instruments) under the control of an IBM-AT computer. The excitation source was through a Coherent Innova 100K krypton laser (406.7 and 413.1 nm). Samples contained in a 5 mm NMR tube were positioned in a backscattering geometry and kept spinning during laser illumination. To minimize the photolysis of the nitrosyl adducts of Mn(II)sGC and Co(II)sGC a cylindrical lens was used to focus the laser beam into a line 0.5 cm in height. The laser power at the sample point was less than 20 mW. All Raman spectra were calibrated with the known frequencies of various solvents whose spectra were recorded before and after the experiments. Spectra were recorded at concentrations of 5−10 μM sGC derivative.

Results

Enzyme Activity Studies. We have measured the activity of heme-depleted and metalloporphyrin-reconstituted sGC to determine the effect of the different metalloporphyrins on sGC function and activation. A comparison of the specific activities (Table 1) shows that the presence of any metalloporphyrin in the heme site of sGC suppresses the basal activity of the enzyme. The suppression of enzyme activity by metalloporphyrins, including the native Fe(II)PPIX, is consistent with previous observations.[15] The metalloporphyrin-reconstituted enzymes, Mn(II)sGC, Fe(II)sGC, and Co(II)sGC, demonstrate remarkably different responsiveness to *S*-nitroso-*N*-acetyl-penicillamine (SNAP), a NO donor (Table 1 and Figure 1). The heme-depleted sGC and Mn(II)sGC are activated minimally by SNAP and to approximately the same extent, 6 and 5-fold, respectively. This observation suggests that Mn(II)PPIX(NO) does not activate sGC; the residual activation observed is due to the small amount of endogenous Fe(II)PPIX remaining after heme-depletion and Mn(II)PPIX-reconstitution. Both Fe(II)sGC and the Co(II)sGC are activated substantially by SNAP, 73 and 101-fold respectively, indicating that Fe(II)PPIX(NO) and Co(II)-PPIX(NO) are both capable of activating sGC. Sodium nitroprusside or gaseous NO produce similar results. Interestingly, Co(II)sGC is activated consistently to a greater extent by NO or NO-donors than Fe(II)sGC.

Table 1. Specific Activity of Heme-Depleted and Metalloporphyrin-Reconstituted sGC with and without NO[a]

protein sample	specific activity without SNAP	specific activity with SNAP
sGC	0.0347	0.199
Mn(II)sGC	0.0270	0.127
Fe(II)sGC	0.0282	2.07
Co(II)sGC	0.0295	2.97

[a] Specific activities are in μmol/min/mg, measured in the presence of natural cofactor Mg^{2+} as described under Materials and Methods. Activation was measured using 100 μM SNAP as the NO donor.

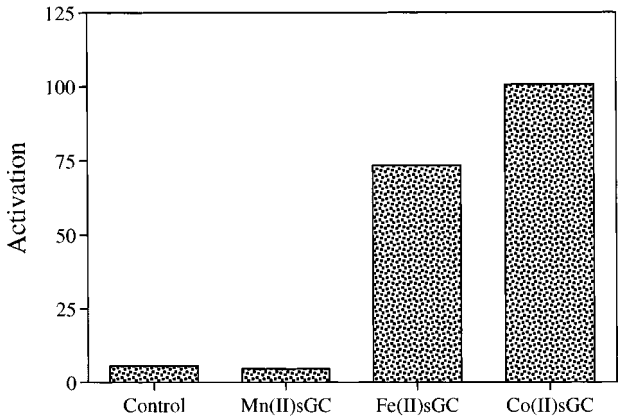

Figure 1. Activation of heme-depleted and metalloporphyrin-reconstituted sGC by NO. Activation of sGC depleted of heme and reconstituted with Mn(II)PPIX, Fe(II)PPIX, and Co(II)PPIX by 100 μM SNAP. Activation is the specific activity of sGC in the presence of activator divided by the specific activity in its absence. Assays were performed as described in the text using the natural cofactor, Mg^{2+}. This graph was generated using the data in Table 1.

Electronic Absorption Spectroscopy. Comparison of the electronic absorption spectral characteristics of Mn(II)PPIX in sGC with those of other Mn-substituted heme proteins and model compounds reveals the nature of the coordination environment of the metal. The spectrum of Mn(II)sGC shows a pronounced blue shift of all the peaks upon addition of NO indicating the formation of Mn(II)sGC(NO) (Figure 2). The peak positions and intensities for the electronic absorption spectra of Mn(II)sGC and Mn(II)sGC(NO) are given in Table 2. The electronic absorption spectra are indicative of incorporation of the Mn(II)PPIX into sGC; the positions of the Soret, α, and β peaks are substantially red-shifted relative to four-coordinate aqueous Mn(II)PPIX (Table 3). The Soret, α, and β peak positions of Mn(II)sGC are comparable to those of other Mn(II)PPIX-reconstituted heme proteins and model compounds known to contain a five-coordinate Mn(II) with one histidine or imidazole ligand (Table 3), implying a similar coordination

(37) de Duve, C. *Acta Chem. Scand.* **1948**, *2*, 264−289.

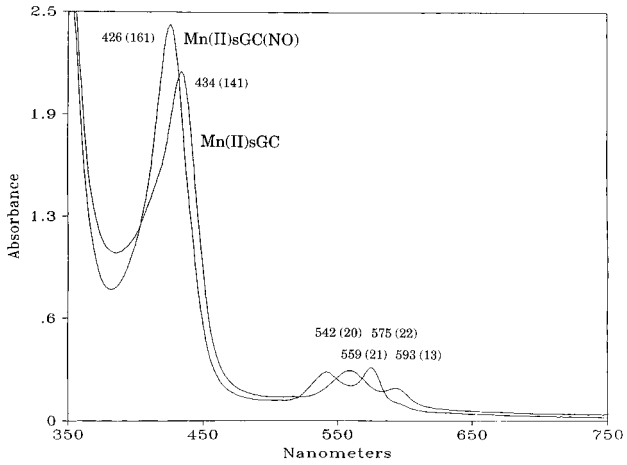

Figure 2. Electronic absorption spectra of Mn(II)sGC and Mn(II)-sGC(NO). The spectra of Mn(II)PPIX-reconstituted sGC (15 μM) with and without 50 μM NO in 25 mM TEA buffer, pH 7.4, 5 mM DTT. Peak positions and molar absorptivities are listed in Table 2.

Table 2. Electronic Absorption Data for Metalloporphyrin-Reconstituted Derivatives of Soluble Guanylyl Cyclase[a]

	peak positions (nm), extinction coefficients (mM^{-1} cm^{-1})		
derivative	Soret (ϵ)	β (ϵ)	α (ϵ)
Mn(II)sGC	434 (141)	559 (21)	593 (13)
Mn(II)sGC(NO)	426 (161)	542 (20)	575 (22)
Co(II)sGC	401 (114)	525 (sh)	560 (19)
Co(II)sGC(NO)	390 (107)	536 (19)	567 (23)

[a] All peak positions are in nm; millimolar absorptivities are in mM^{-1} cm^{-1}. All values were determined in 25 mM TEA buffer, pH 7.4, 5 mM DTT. Extinction coefficients were calculated based on Mn and Co concentrations measured by atomic absorption spectrophotometry.

Table 3. Comparison of Electronic Absorption Spectral Characteristics of MnPPIX Compounds and Various MnPPIX-Reconstituted Heme Proteins

	peak positions (nm)				
protein/species	Soret	β	α		ref
Mn(III)PPIX	370	465	555		47
Mn(III)CCP	377	483	568	605	47, 48
Mn(III)HRP	373	482	564	584	47
Mn(III)Mb	374	471	556		47
Mn(III)Hb	382	476	553		48
Mn(II)PPIX, aqueous	420	547	577		47
Mn(II)PPIX(2-MeImH)	428	556	588		40
Mn(II)CCP	439	563	595		47, 48
Mn(II)Mb	438	560	598		40, 47
Mn(II)Hb	444	557	600		40, 48
Mn(II)sGC	434	559	593		this work
Mn(II)Hb(NO)	433	538	580		48
Mn(II)CCP(NO)	427	543	572		48
Mn(II)sGC(NO)	426	542	575		this work

environment for Mn(II) in sGC. The peak positions of Mn-(II)sGC(NO) are very similar to those of the NO-adducts of Mn(II)PPIX-reconstituted Hb and CCP, proteins known to contain six-coordinate Mn(II) with both the proximal His and NO bound to the manganese atom (Table 3). The similarity between the spectra of Mn(II)sGC and Mn(II)sGC(NO) and those of analogous derivatives of Hb, Mb, and CCP suggests that Mn(II)sGC is five-coordinate with only the proximal His bound to Mn, while Mn(II)sGC(NO) is six-coordinate with both the proximal His and NO bound.

Similar analysis of the electronic absorption spectra of Co-(II)sGC and Co(II)sGC(NO) provides information as to the coordination environment of Co(II)PPIX in sGC. Peak positions and extinction coefficients for Co(II)sGC and Co(II)sGC(NO) are given in Table 2. The spectral shifts upon binding NO to Co(II)sGC are similar to those observed in the reaction of the model compound Co(II)OEP with NO in CH_2Cl_2 (spectrum not shown). The spectral characteristics of both Co(II)sGC and Co-(II)sGC(NO) were closer to those of the five-coordinate Co-(II)Hb and Co(II)Mb than to those of the six-coordinate Co(II) cytochrome *c* (Table 4), indicating that Co(II)sGC is five-coordinate with only the proximal His bound. The similarity between the spectral changes observed upon NO adduct formation in Co(II)OEP and Co(II)sGC suggest that a similar NO adduct is formed in both cases. Since there is no available exogenous ligand save NO, Co(II)OEP(NO) must be five-coordinate, and the spectral similarities therefore suggest that Co(II)sGC(NO) is also five-coordinate.

Table 4. Comparison of Electronic Absorption Spectral Characteristics of Various CoPPIX-Reconstituted Heme Proteins

	peak positions (nm)			
protein	Soret	β	α	ref
Co(II)Mb	406	523 (sh)	558	49
Co(II)Hb	402	523 (sh)	552	49
Co(II)cyt c	416.5	520 (sh)	549	50
Co(II)sGC	401	525 (sh)	560	this work

Table 5. Comparison of the Soret Absorption Maxima for $Fe^{II}NO$, $Co^{II}NO$, and $Mn^{II}NO$ Heme Proteins and Models

protein/species	Soret band (nm)	coordination state	ref
Co(II)PPIX(py)(NO)	422	six-coordinate	this work
Co(II)OEP(Im)(NO)/CH_2Cl_2	426	six-coordinate	this work
Co(II)OEP(NO)/CH_2Cl_2	394	five-coordinate	this work
Co(II)PPIX(NO), aqueous	395	five-coordinate	this work
Co(II)sGC(NO)	390	five-coordinate	this work
Fe(II)PPIXDME(1-MeIm)(NO)	415	six-coordinate	51
Fe(II)Mb(NO)	422	six-coordinate	51
Fe(II)$P450_{cam}$	439	six-coordinate	53
Fe(II)PPIXDME(NO)/toluene	398	five-coordinate	19
Fe(II)sGC(NO)	398	five-coordinate	18,19
Mn(II)Hb(NO)	433	six-coordinate	48
Mn(II)CCP(NO)	427	six-coordinate	48
Mn(II)OEP(NO)/CH_2Cl_2	396	five-coordinate	this work
Mn(II)PPIX(NO)/aqueous	414	five-coordinate	this work
Mn(II)sGC(NO)	426	six-coordinate	this work

Comparison of the spectral position of the Soret absorption maxima in both manganese and cobalt porphyrin nitrosyl models and nitrosyl manganese and cobalt substituted hemoproteins provides further support for the formation of the NO adducts and for their respective coordination geometries. As illustrated in Table 5, the five coordinate nitrosyl complexes exhibit Soret maxima that are significantly blue shifted relative to the related six-coordinate complexes. Typically, the binding of a sixth ligand to these metalloporphyrin nitrosyl species results in a >10 nm shift in the Soret absorption maximum to longer wavelengths. This trend is seen in all the metalloporphyrin models and non-native metallosubstituted proteins studied and provides strong evidence for the coordination geometry of the nitrosyl adducts. Comparison of the data for Mn(II)sGC and Co(II)sGC with those for other systems strongly suggests that Mn(II)sGC(NO) is six-coordinate while Co(II)sGC(NO) is five-coordinate.

Resonance Raman Spectroscopy. To further probe the coordination structure of Mn(II)sGC and Co(II)sGC, we have obtained the RR spectra of these metalloporphyrin-substituted proteins (Figure 3). Table 6 compares the RR frequencies of two marker bands (ν_3 and ν_4) for Mn(II)sGC and Co(II)sGC with those of some relevant model systems. These two modes have been established to be reliable marker bands for the oxidation and spin states as well as for the coordination

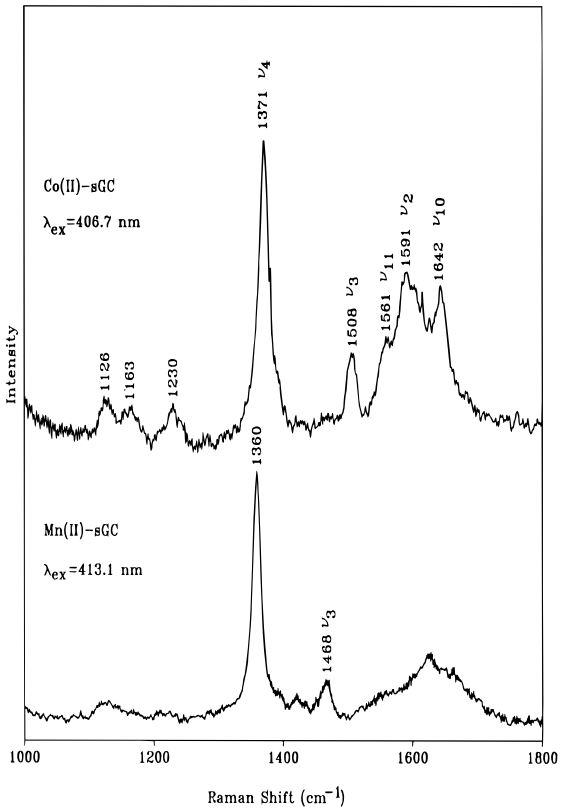

Figure 3. High frequency resonance Raman spectrum of Mn(II)sGC and Co(II)sGC. The spectrum of Mn(II)PPIX- and Co(II)PPIX-reconstituted sGC in 25 mM TEA buffer, pH 7.4, 5 mM DTT. The positions of key vibrational modes are tabulated in Table 6 for comparison with other proteins.

Table 6. Comparison of Resonance Raman Spectral Characteristics for Mn(II)PPIX- and Co(II)PPIX-Reconstituted Heme Proteins and Models

protein/species	ν_3 (cm^{-1})	ν_4 (cm^{-1})	ref
Mn(II)sGC	1468	1359	this work
Mn(II)Hb	1463	1356	40
Mn(II)Mb	1466	1356	40
Mn(II)PPIX(2-MeImH)	1464	1357	40
Co(II)sGC	1508	1374	this work
Co(II)Hb	1508	1373	41
Co(II)Mb	1508	1373	41
Co(II)PPIX(Pip)	1508	1373	41
Co(II)PPIX(Py)	1506	1374	41

environments of the central metal ions. For Mn-porphyrins, ν_4 is known to occur at about 1370 and 1360 cm^{-1} for Mn(III) and Mn(II), respectively. Thus, it is apparent that MnPPIX has been successfully reconstituted into sGC in the Mn(II) state, since ν_4 is observed at 1359 cm^{-1}. The coordination state of Mn(II) is inferred to be five-coordinate from the frequency of ν_3 (1468 cm^{-1}) for Mn(II)sGC. The observation of five-coordination in both the electronic absorption and RR spectra is indicative of the incorporation of the porphyrin into the protein. Mn(II)PPIX in aqueous solution is four-coordinate, exhibiting a ν_3 frequency at 1438 cm^{-1}; when Mn(II)PPIX becomes five-coordinate in the presence of 2-MeIm ν_3 is shifted to 1464 cm^{-1}.[40] Nearly the same frequency is also observed for Mn(II)Mb (1466 cm^{-1}) and Mn(II)Hb (1463 cm^{-1}), in which Mn(II) is known to be in the five-coordinate state. Thus, both the electronic absorption and RR data are consistent and reveal that Mn(II)sGC is five-coordinate with histidine as a likely axial ligand.

High and low frequency RR spectra of Co(II)sGC are less informative than those of Mn(II)sGC, although evidence for the incorporation of CoPPIX in the +2 oxidation state is obtained. As the peak positions for the marker bands in the Co(II)sGC spectrum match those of Co(II) model compounds (Table 6), it is clear that the metal is in the +2 oxidation state. The porphyrin marker bands ν_3 and ν_4 are uninformative about the coordination state of the Co(II), in contrast to Mn(II). These modes occur between 1510−1511 cm^{-1} (ν_3) and 1374−1378 cm^{-1} (ν_4) for the four-coordinate models Co(II)PPIX, Co(II)-PPIXDME, and Co(II)OEP, consistent with earlier work of Woodruff et al.[41] who found no significant shifts in the high frequency modes of the five-coordinate and six-coordinate cobalt proteins and models.

We attempted unsuccessfully to acquire the RR spectra of the NO adduct of Mn(II)sGC. The 413.1-nm excitation spectra of Mn(II)sGC(NO) (not shown) are invariably the same as that of Mn(II)sGC; electronic absorption spectra recorded immediately before and after the RR spectrum are characteristic of Mn(II)sGC(NO). These observations reveal that the bound NO is reversibly photolyzed in the laser beam. Attempts to avoid the photolysis by attenuating the incident laser power were unsuccessful; even with a cylindrical lens at 1 mW of laser power, the RR bands were characteristic of Mn(II)sGC. The NO-off photostationary state of the NO adduct for Mn(II)sGC is in contrast to other NO adducts of Mn(II)porphyrins and Mn-(II)PPIX-reconstituted Mb and Hb, for which RR spectra can be obtained.[42] Although the quantum yield for ligand photodissociation in PMn(II)NO is ∼1,[43,44] Parthasarathi and Spiro[42] have observed variations in the apparent photolability (i.e., the position of the photostationary state) among Mn(II)Hb(NO), Mn(II)Mb(NO), and Mn(II)PPIXDME(pip)(NO) which they attribute to changes in the conformation of protein residues in the heme pocket. The apparent photolability of Mn(II)sGC-(NO) therefore suggests a unique heme-binding environment for the six-coordinate Mn(II)sGC(NO) complex and implies that the heme stereoelectronic environment is capable of modulating NO binding in non-native forms of the protein.

The coordination environment of Co(II)sGC(NO) can readily be deduced from the frequencies of the bound NO vibrations, which appear in the RR spectra. Figure 4 shows the high frequency RR spectra of the NO adduct for Co(II)sGC, prepared by the autoreduction of Co(III)sGC in the presence of NO. The binding of NO to Co(II) is evident from the upshift of ν_4 from 1370 cm^{-1} for Co(II)sGC (Figure 3) to 1377 cm^{-1} in Co(II)-sGC(NO) (Figure 4). In order to locate the $\nu_{(N-O)}$ mode, expected in the frequency region of 1600−1800 cm^{-1}, we acquired a RR spectrum of the ^{15}NO adduct under the same experimental conditions. Close examination of these two spectral traces shows a slight intensity decrease at 1675 cm^{-1} for natural abundance NO and an obvious intensification for a spectral feature centered at 1638 cm^{-1}. When both traces are normalized by using the ν_4 band as an internal intensity standard and trace B is subtracted from trace A, a difference spectrum (trace C) is obtained. The positive and negative features in the difference spectrum clearly identify the N−O stretching mode. The ^{15}N isotopic shift (37 cm^{-1}) agrees with the calculated shift

(38) Garbers, D. L.; Murad, F. *Adv. Cyclic Nucleotide Res.* **1979**, *10*, 57−67.

(39) *Hawk's Physiological Chemistry*, 14th ed.; Oser, B. L., Ed.; McGraw Hill: New York, 1965; pp 178−181.

(40) Parthasarathi, N.; Spiro, T. G. *Inorg. Chem.* **1987**, *26*, 3792−3796.

(41) Woodruff, W. H.; Adams, D. H.; Spiro, T. G.; Yonetani, T. *J. Am. Chem. Soc.* **1975**, *97*, 1695−1698.

(42) Parthasarathi, N.; Spiro, T. G. *Inorg. Chem.* **1987**, *26*, 2280−2282.

(43) Hoffman, B. M.; Gibson, Q. H. *Proc. Natl. Acad. Sci. U.S.A.* **1978**, *75*, 21−25.

(44) Gibson, Q. H.; Hoffman, B. M. *J. Biol. Chem.* **1979**, *254*, 4691−4697.

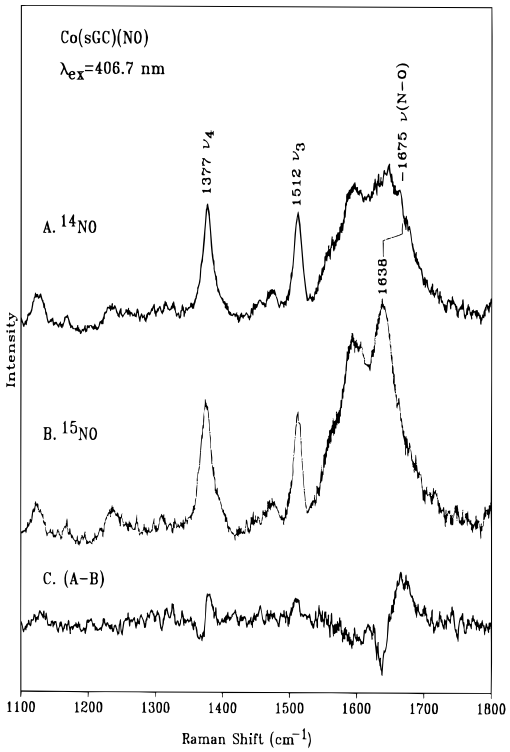

Figure 4. High frequency resonance Raman spectra of the NO adduct of Co(II)sGC and its ^{15}NO isotopomer. The spectra of Co(II)PPIX-reconstituted sGC with 50 μM ^{14}NO and 50 μM ^{15}NO in 25 mM TEA buffer, pH 7.4, 5 mM DTT: (A) Co(II)sGC(^{14}NO), (B) Co(II)sGC-(^{15}NO), and (C) A-B. The positions of key vibrational modes are given in Table 7.

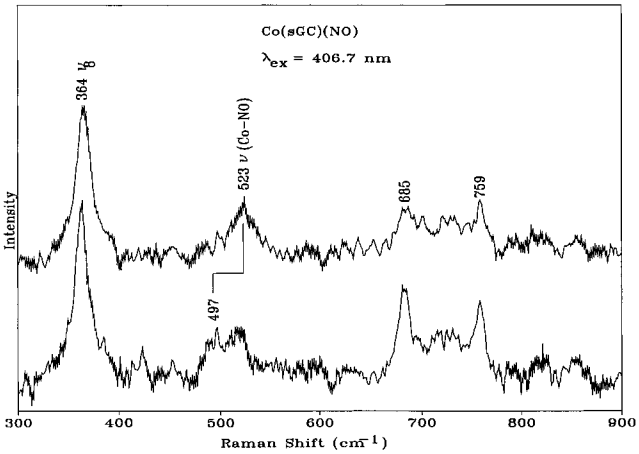

Figure 5. Low frequency resonance Raman spectra of the NO adduct of Co(II)sGC and its ^{15}NO isotopomer. The spectra of Co(II)PPIX-reconstituted sGC with 50 μM ^{14}NO and 50 μM ^{15}NO in 25 mM TEA buffer, pH 7.4, 5 mM DTT: (A) Co(II)sGC(^{14}NO), (B) Co(II)sGC-(^{15}NO). The positions of key vibrational modes are given in Table 7.

(31 cm^{-1}) for a two-body vibrator. The low frequency region of the RR spectra for Co(II)sGC(NO) is expected to contain the $\nu_{(Co-NO)}$ vibration. As is shown in Figure 5, a prominent feature (centered at 523 cm^{-1}) is found to be sensitive to ^{15}N-isotope substitution, shifting to 497 cm^{-1}, and is assigned to $\nu_{(Co-NO)}$ by analogy with the NO adducts of Co(II)Mb and Co-(II)Hb. A band at 516 cm^{-1} underlies the 523 cm^{-1} band and is revealed in the ^{15}N spectrum. This band arises from a nearby porphyrin mode.[45]

The $\nu_{(N-O)}$ and $\nu_{(Co-NO)}$ frequencies are markedly different for five- and six-coordinate NO adducts of Co(II) porphyrins (Table 7). Co(II)sGC(NO) exhibits essentially the same frequencies, 1675 and 523 cm^{-1}, as the five-coordinate model complexes Co(II)OEP(NO) (1672 and 521 cm^{-1}) and Co(II)-PPIXDME(NO) (1678 and 519 cm^{-1}) dissolved in methylene chloride and Co(II)PPIX(NO) (1675 and 528 cm^{-1}) dissolved in dilute NaOH. Spectra of the Co(II)OEP(NO) model complex are presented in Figures 6 and 7. In Co(II)Hb(NO) and Co-(II)Mb(NO), $\nu_{(N-O)}$ is at lower frequency (1620 and 1614 cm^{-1}, respectively) and $\nu_{(Co-NO)}$ is at higher frequency (566 and 576 cm^{-1}) than in Co(II)sGC(NO). These shifts are attributable to coordination by the proximal histidine in the globins and may also reflect distal interactions.[46] Clearly, these data reveal that the proximal histidine is not bound in Co(II)sGC(NO).

Table 7. Comparison of Resonance Raman Spectral Characteristics for the Nitrosyl Adducts of CoPPIX-Reconstituted Heme Proteins and Models

	vibrational mode (cm^{-1})			
protein/species	ν_4	ν_{NO}	ν_{Co-NO}	ref
Co(II)sGC(NO)	1377	1675	523	this work
Co(II)Hb(NO)	1378	1620	566	52
Co(II)Mb(NO)	1378	1614	576	52
Co(II)OEP(NO)/CH_2Cl_2	1376	1672	521	this work
Co(II)PPIX(NO)/NaOH	1379	1675	528	this work
Co(II)PPIXDME(NO)/CH_2Cl_2	1378	1678	519	this work

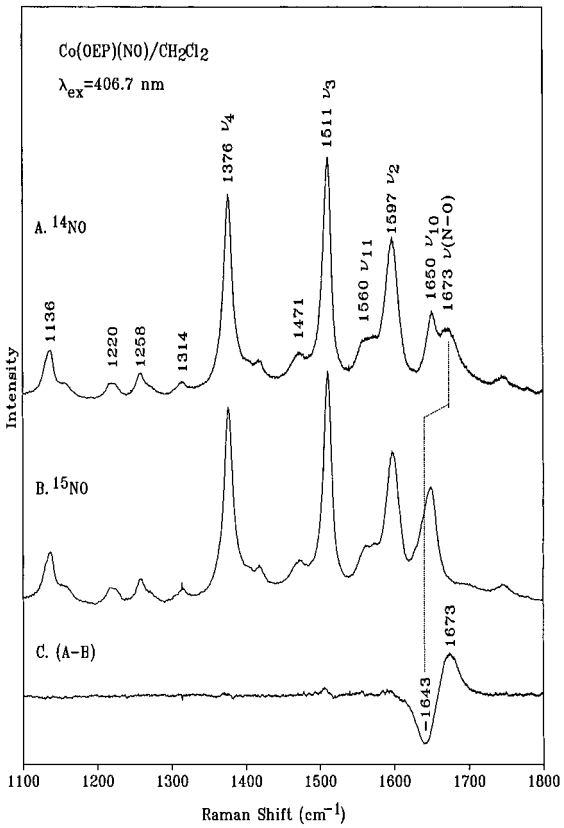

Figure 6. High frequency resonance Raman spectra of the NO adduct of Co(II)OEP and its ^{15}NO isotopomer. The spectra of the nitric oxide adduct of Co(II)OEP in dichloromethane: (A) Co(II)OEP(^{14}NO), (B) Co(II)OEP(^{15}NO), and (C) A-B. The positions of key vibrational modes are given in Table 7.

Discussion

Activation of soluble guanylyl cyclase is a key step in the physiological function of NO. Although it has been known for

(45) Li, X.-Y.; Czernuszewicz, R. S.; Kincaid, J. R.; Stein, P.; Spiro, T. G. *J. Chem. Phys.* **1990**, *94*, 47−61.
(46) Yu, N. T.; Thompson, H. M.; Mizukami, H.; Gersonde, K. *Eur. J. Biochem.* **1986**, *159*, 129−132.

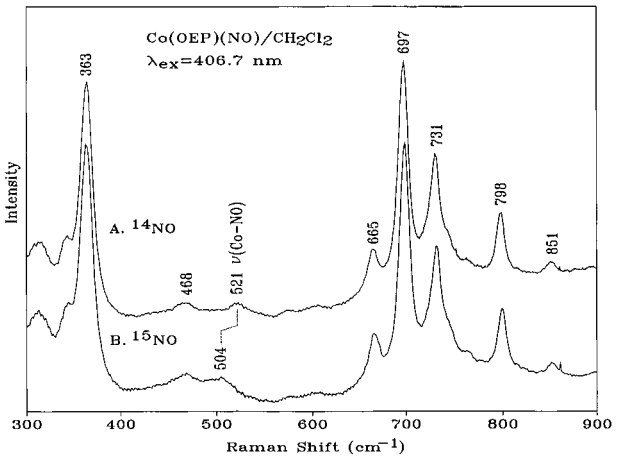

Figure 7. Low frequency resonance Raman spectra of the NO adduct of Co(II)OEP and its ^{15}NO isotopomer. The spectra of the nitric oxide adduct of Co(II)OEP in dichloromethane: (A) Co(II)OEP(^{14}NO), (B) Co(II)OEP(^{15}NO). The positions of key vibrational modes are given in Table 7.

some time that the heme in sGC was intimately involved in the activation process, an understanding of the molecular mechanism of NO action on sGC has only recently evolved. Ignarro and co-workers[2] noted that the free-base porphyrin and NO-heme activated sGC give kinetically indistinguishable forms of the enzyme. The heme-deficient protein was kinetically competent to convert GTP to cGMP, but only at a slow, basal rate, whereas reconstitution with nitrosylheme resulted in full activation of the enzyme.[2] Later calculations[25] and model studies[26] by Traylor and Sharma emphasized that dissociation of an axial ligand is an intrinsic aspect of NO binding to histidine-ligated heme model complexes. Spectroscopic studies have conclusively demonstrated that NO-activated sGC contains a five-coordinate nitrosyl heme, Fe(II)PPIX(NO),[18,19,21,22] while the resting state is either a mixture of five-coordinate and six-coordinate Fe(II)PPIX with His axial ligand(s)[19,20] or five-coordinate[18,22] with a single axial His. The CO-adduct of sGC is six-coordinate with the proximal His bound[18−20,22,27] and is not activated at physiological levels of CO.[20] These data are consistent with a model in which both the scission of metal-axial ligand bond trans to the NO and the presence of the porphyrin in the heme-binding pocket are required for activation of sGC.

We have set out to test the hypothesis that activation correlates with the scission of the proximal-histidine to iron bond through metalloporphyrin reconstitution experiments. Existing structural studies[28−33] by Scheidt and co-workers using Mn(II), Fe(II), and Co(II) porphyrin complexes have demonstrated an increasing trans influence across the first row transition metals from Mn(II) to Co(II) in the presence of a nitrosyl ligand. The metal−axial ligand bond trans to NO lengthens from Mn(II) to Fe(II); six-coordinate Fe(II) porphyrin nitrosyls exhibit substantial elongation of the metal−ligand bond trans to NO,[28] while analogous Mn(II) complexes show no trans influence.[29,30] The five-coordinate complexes, Fe(II)TPP(NO)[33] and Co(II)TPP(NO),[31] were also crystallized, and it was noted that the Fe−NO bond was shorter than the Co−NO bond, indicative of poorer back-bonding in the Co−NO adduct. Co(II) porphyrin nitrosyls could not be crystallized with a sixth ligand;[31] the presence of the NO apparently rendered the six-coordinate complexes unstable. Based on the known model structures and the proposed activation mechanism, we anticipated that Mn(II)sGC(NO) would be six-coordinate with the proximal His bound and would not be activated and that Co(II)sGC(NO) would be five-coordinate. Scission of the proximal metal-His bond in Co(II)sGC(NO) should result in activation of the enzyme.

Scheme 1. Structurally Characterized Non-Native Forms of sGC: A. the Structural Changes Associated with Binding NO to Mn(II)sGC and B. the Structural Changes Associated with Binding NO to Co(II)sGC

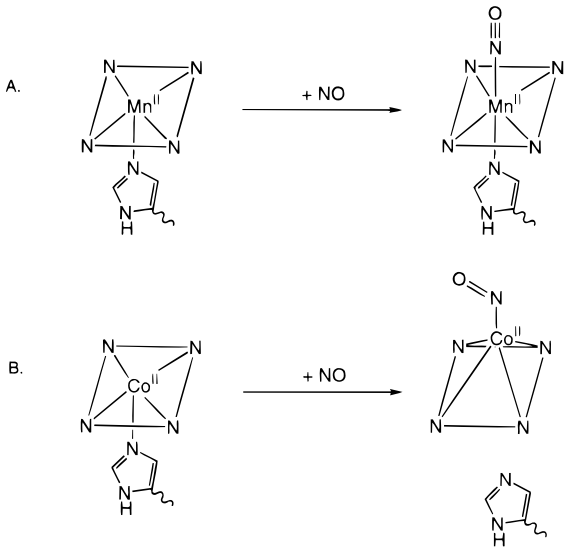

Spectroscopic characterization of the metalloporphyrin-reconstituted enzymes confirms the predicted structure for the NO adducts and provides further support for the presence of histidine as the axial ligand in sGC. The structures of these non-native forms of sGC are illustrated in Scheme 1. Both Mn(II)PPIX and Co(II)PPIX were readily introduced into sGC, and in both cases the resulting complexes were five coordinate, as revealed by comparison of the electronic absorption and resonance Raman spectra of Mn(II)sGC with those of model complexes and other Mn(II)PPIX-reconstituted proteins.[47,48] The electronic absorption and RR spectra of Mn(II)sGC are very similar to those of Mn(II)PPIX(2-MeIm), Mn(II)Hb, and Mn(II)Mb, which are all known to be five-coordinate. Similarly, the electronic absorption and RR spectra of Co(II)sGC are consistent with a five-coordinate structure in which an axial histidine is bound to cobalt. The electronic absorption spectrum of Co(II)sGC is very similar to the spectra of Co(II)Hb and Co(II)Mb[49] and distinctly different in the position of the Soret maximum from the six-coordinate complex formed in Co(II)-cyt *c*.[50] Together, the similarity between Mn(II)sGC and Co(II)sGC and the analogous Hb and Mb derivatives provides further evidence for the presence of an axial histidine ligand in sGC.

The spectral changes observed are consistent with the formation of NO adducts with the non-native metalloporphyrin-substituted sGC. Five-coordinate NO adducts of Mn, Co, and Fe porphyrins are characterized by blue shifted Soret absorption maxima, while the related six-coordinate NO adducts are characterized by red-shifted Soret maxima. The electronic absorption spectrum of Mn(II)sGC(NO) exhibits a Soret maximum at 426 nm, similar to Mn(II)CCP(NO),[48] and is consistent

(47) Yonetani, T.; Asakura, T. *J. Biol. Chem.* **1969**, *244*, 4580−4588.
(48) Yonetani, T.; Yamamoto, H.; Erman, J. E.; Leigh, J. S. J.; Reed, G. H. *J. Biol. Chem.* **1972**, *247*, 2447−2455.
(49) Yonetani, T.; Yamamoto, H.; George V. Woodrow, I. *J. Biol. Chem.* **1974**, *249*, 682−690.
(50) Dickenson, L. C.; Chien, J. C. W. *Biochemistry* **1975**, *14*, 3526−3534.
(51) Romberg, R. W.; Kassner, R. J. *J. Am. Chem. Soc.* **1979**, *18*, 5387−5392.

with six-coordination. When NO is added to Mn(II)sGC, the Soret maximum shifts to shorter wavelength by approximately 10 nm, from 434 to 426 nm, while the α and β maxima blue-shift by nearly 20 nm. These shifts are reminiscent in both magnitude and direction to those observed when NO reacts with both Mn(II)Hb and Mn(II)CCP.[48] Electronic spectral characterization of Co(II)sGC(NO) reveals that this species contains a five-coordinate cobalt nitrosyl porphyrin, characterized by a Soret maximum at 390 nm. The electronic absorption spectrum of Co(II)sGC shows a blue shift of the Soret and a red shift of the α and β peaks upon addition of NO and greater definition of the β peak in Co(II)sGC(NO) than in the Co(II)sGC. These spectral changes are similar to those observed for the addition of NO to Co(II)OEP to form five-coordinate Co(II)OEP(NO). In the RR spectrum of Co(II)sGC(NO) the $\nu_{(NO)}$ and $\nu_{(Co-NO)}$ vibrational modes are found at distinctly different frequencies from those observed for six-coordinate Co(II)Hb(NO) and Co(II)Mb(NO).[51] The positions of $\nu_{(NO)}$ and $\nu_{(Co-NO)}$ modes for Co(II)sGC(NO) are very similar to those of the five-coordinate model compounds, Co(II)OEP(NO), Co(II)PPIX(NO), and Co(II)PPIXDME(NO), implying that Co(II)sGC(NO) is five-coordinate with no protein ligand bound.

The activity of the protein correlates as predicted with the coordination structure of the metalloporphyrin, providing confirmation of the validity of the proposed activation mechanism. When a metalloporphyrin, Mn(II)PPIX, Co(II)PPIX, or the native Fe(II)PPIX, is bound in the heme site the activity of the enzyme is depressed relative to the heme-free form. This unactivated state occurs when the axial histidine ligand is bound to the metal ion in the metalloporphyrin. Similarly, in the cases of Fe(II)sGC(CO) or Mn(II)sGC(NO) where the axial histidine remains bound, the enzyme is in the unactivated state. Only when the axial ligand is released from the metal does the enzyme achieve the fully activated state. Thus Fe(II)sGC(NO) and Co(II)sGC(NO), both of which are five-coordinate, are substantially activated. We have noted that Co(II)sGC(NO) is consistently activated to a greater extent that Fe(II)sGC(NO), an observation that we hypothesize arises due to the predicted greater thermodynamic instability of the metal-proximal histidine bond in the cobalt enzyme.

Importantly, the enzyme is not activated in the complete absence of heme but is activated by the free-base porphyrin. Ignarro and co-workers[15,16] demonstrated that activation by the free-base porphyrin, PPIX, is competitively inhibited by FePPIX, suggesting that both species are binding to an unique heme site on the enzyme. The inability of the metal-free porphyrin to bind the axial histidine ligand correlates with its ability to activate the enzyme. The observation that heme-free sGC is not activated but PPIX-reconstituted sGC is activated implies that the heme periphery must also play a key role in the activation of sGC. Therefore, the absence of a metal−proximal histidine bond is a necessary but not sufficient criterion for activation of sGC.

Scheme 2. Model for Allosteric Regulation of Activity in sGC via Scission of the Iron−Proximal Histidine Bond

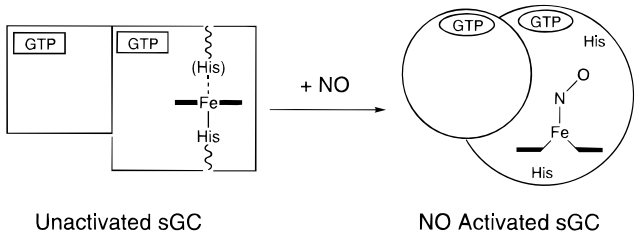

The results of this study support a mechanism for sGC activation in which the scission of the metal−proximal histidine bond occurs upon NO binding to the heme. By taking advantage of the trans influence in the NO-adducts of metalloporphyrins, we have created new non-native forms of sGC in both the activated (Co(II)sGC(NO)) and unactivated (Mn(II)sGC(NO)) states. These results demonstrate that it is possible to modulate the activity of sGC in predictable ways through changes in the coordination structure of the heme or metalloporphyrin and clearly implicate scission of the metal−proximal histidine bond in activation of sGC. A model for the activation of sGC which is consistent with these data and those of others is illustrated in Scheme 2. In this model, the formation and scission of the metal−proximal histidine bond allows the protein to interconvert between activated and unactivated conformations. Allosteric control of conformation via changes in the coordination environment of a metal ion has ample precedent in the cooperative binding of dioxygen to hemoglobin and may provide a broad paradigm for sensors of small gaseous molecules.

Acknowledgment. This work was supported in part by Grant HL-54762 from the National Institutes of Health (J.N.B.), a Grant-in-Aid from the American Heart Association (J.N.B.), the Wisconsin Alumni Research Foundation (J.N.B.), and by Grants GM33576 and GM17278 from the National Institutes of Health (T.G.S.). Fellowship support from the Alfred P. Sloan Foundation (J.N.B.), the NIH Biotechnology Training Grant (E.A.D.), the Department of Education (A.E.Y.), and a NIH National Research Service Award (K.M.V.) are gratefully acknowledged. J. N. B. thanks Dr. Robert Petrovich for valuable discussions.

JA9603057

(52) Hu, S. *Inorg. Chem.* **1993**, *32*, 1081−1085.
(53) Hu, S.; Kincaid, J. R. *J. Am. Chem. Soc.* **1991**, *113*, 9760−9766.